

Detection capability of teleseismic events recorded at Syowa Station, Antarctica: 1987–2007

Masaki Kanao^{1,2*}

南極・昭和基地における遠地地震の検知率 —1987～2007—

金尾政紀^{1,2*}

(Received November 13, 2009; Accepted January 25, 2010)

要旨: 南極・昭和基地 (69.0° S, 39.6° E) では、短周期、長周期の各3成分のアナログ及びデジタル記録による地震記象の読み取り作業が、1967年以降現在まで継続されている。インテルサット衛星回線の導入に伴い、2005年度以降は国立極地研究所へ自動伝送されたデジタルデータを用いた読み取りも併用している。P, PKP, PP, S, SKS等の地震波走時と震源データは、アメリカ地質調査所 (USGS) と国際地震センター (ISC) へ定期的に送られると共に、“JARE Data Reports (Seismology)”として発刊されている。本稿では、1987年より2007年の21年間における験震データを用いて、昭和基地の地震モニタリング観測で記録された遠地地震の空間分布と時間的推移を調べた。特に震源パラメータについて、地震の深さ依存性やマグニチュード検知レベルの季節変動を考察した。またISCデータを用いたグローバル観測網の結果と比較して、南半球の地震検知率について議論した。

Abstract: A phase identifying procedure for the teleseismic events at Syowa Station (69.0° S, 39.6° E), Antarctica has been carried out since 1967 by use of analog and digital records of short- and long-period seismometers. After the establishment of an INTELSAT telecommunication link, several kinds of digital data have been transmitted to the National Institute of Polar Research (NIPR) for the utilization of seismic phase identification. The arrival times of several phases, such as P, PKP, PP, S, SKS have been reported to the United States Geological Survey (USGS) and International Seismological Center (ISC), then published as the “JARE Data Reports (Seismology)”. In this paper, hypocentral distribution and time variations for the detected earth-

¹ 情報・システム研究機構国立極地研究所。National Institute of Polar Research, Research Organization of Information and Systems, Midoricho 10-3, Tachikawa, Tokyo 190-8518.

² 総合研究大学院大学複合科学研究科極域科学専攻。Department of Polar Science, School of Multidisciplinary Sciences, The Graduate University for Advanced Studies (SOKENDAI), Midoricho 10-3, Tachikawa, Tokyo 190-8518.

* Corresponding author. E-mail: kanao@nipr.ac.jp.

quakes by monitoring observation at Syowa Station was studied in the 21 year period from 1987 to 2007 by using the published Data Reports. The epicentral parameters were investigated in terms of focal depth dependency and seasonal trending in the threshold range of detectable magnitude. Moreover, the detection capability of teleseismic events in the southern hemisphere was discussed in comparison with global results derived from ISC data.

1. Introduction

As a contribution to global seismographic network, seismic phase identification by calculating the travel-times of teleseismic events at Syowa Station (69.0° S, 39.6° E), Antarctica, has been carried out since 1967 (Kaminuma *et al.*, 1968). By using analog and digital records from short- and long-period seismometers, the phase identification procedure was continued until 2005 by wintering members for geophysics of the Japanese Antarctic Research Expedition (JARE). After the conclusion of observations by the corresponding wintering party, the identified teleseismic events were re-scaled in the National Institute of Polar Research (NIPR) by the manner described in Chapter 2.

Internet utilization at Syowa Station has significantly advanced since 2005 via the INTELSAT telecommunication system (Kanao *et al.*, 2006a). Since 2005, the phase identification procedure has been conducting only at NIPR by the special staff of the Polar Data Center (PDC). All information on arrival times of the detected seismic phases has been reported to the United States Geological Survey (USGS) and the International Seismological Center (ISC), and published in the “JARE Data Reports (Seismology)” for every year (*e.g.*, Kanao, 1994a; Kanao, 1999; Doi and Kanao, 2006; Iwano and Kanao, 2009). Details of major transitions in the seismic observation system at Syowa Station for these two decades can be referred to Kanao and Kaminuma (1993), Kanao *et al.* (1999) and Kanao *et al.* (2006a). The recently published Data Reports, moreover, described minor changes in the observation system.

By using travel-time data on detected seismic phases together with waveform data recorded at Syowa Station and other permanent / temporary stations in Antarctica, several remarkable studies have been conducted on the heterogeneous structure and dynamics of the Antarctic continent (Kanao *et al.*, 2002; Kuge and Fukao, 2005), on the surrounding oceanic plate (Tsuboi *et al.*, 2000; Kobayashi and Zhao, 2004; Nawa *et al.*, 2007), on local and regional seismic activities (Kanao and Kaminuma, 2006; Kanao *et al.*, 2006b), on the structure and dynamics of the Earth’s deep interior such as the D” zone (Usui *et al.*, 2005; Usui *et al.*, 2008), and on the outer- and inner-cores (Isse and Nakanishi, 2001).

In this paper, the spatial distribution and time variations for detection capability at Syowa Station were studied by using the teleseismic events reported by “JARE Data Reports” for the 21 years 1987–2007 (Akamatsu and Kaminuma, 1989; Kaminuma and Ichikawa, 1990; Kaminuma and Murakami, 1991; Kaminuma and Nagasaka, 1992; Kaminuma and Yamamoto, 1993; Kanao, 1994a; Okano and Kanao, 1995; Nawa and Kanao, 1996; Tanaka and Kanao, 1997; Nogi *et al.*, 1997; Kanao, 1999; Tono and Kanao, 1999; Nakanishi and Kanao, 2001; Seo and Kanao, 2002; Ito

Table 1. Number of detected teleseismic events at Syowa Station for the 21 year period from 1987 to 2007, together with corresponding JARE parties. The total number of events reported in these Data Reports is 19145. Notice the four year period from 1987 to 1990 (denoted by ‘*’ in the corresponding Data Reports); a more critical re-scaling procedure was conducted and modified arrival times and epicenters were listed by Kanao (1995).

Year	Number	JARE party	Reference
1987	393	JARE-27 (January), JARE-28 (February-December)	*Akamatsu and Kaminuma (1989)
1988	489	JARE-28 (January), JARE-29 (February-December)	*Kaminuma and Ichikawa (1990)
1989	788	JARE-29 (January), JARE-30 (February-December)	*Kaminuma and Murakami (1991)
1990	820	JARE-30 (January), JARE-31 (February-December)	*Kaminuma and Nagasaka (1992)
1991	409	JARE-31 (January), JARE-32 (February-December)	Kaminuma and Yamamoto (1993)
1992	614	JARE-32 (January), JARE-33 (February-December)	Kanao (1994)
1993	789	JARE-33 (January), JARE-34 (February-December)	Okano and Kanao (1995)
1994	727	JARE-34 (January), JARE-35 (February-December)	Nawa and Kanao (1996)
1995	896	JARE-35 (January), JARE-36 (February-December)	Tanaka and Kanao (1997)
1996	840	JARE-36 (January), JARE-37 (February-December)	Nogi, Negishi and Kanao (1997)
1997	413	JARE-37 (January), JARE-38 (February-December)	Kanao (1999)
1998	847	JARE-38 (January), JARE-39 (February-December)	Tono and Kanao (1999)
1999	914	JARE-39 (January), JARE-40 (February-December)	Nakanishi and Kanao (2000)
2000	701	JARE-40 (January), JARE-41 (February-December)	Seo and Kanao (2002)
2001	1,418	JARE-41 (January), JARE-42 (February-December)	Ito and Kanao (2003)
2002	1,059	JARE-42 (January), JARE-43 (February-December)	Yoshii and Kanao (2004)
2003	783	JARE-43 (January), JARE-44 (February-December)	Horiuchi and Kanao (2005)
2004	1,664	JARE-44 (January), JARE-45 (February-December)	Doi and Kanao (2006)
2005	1,702	JARE-45 (January), JARE-46 (February-December)	Sakanaka, Uemura and Kanao (2007)
2006	1,608	JARE-46 (January), JARE-47 (February-December)	Chida and Kanao (2009)
2007	1,271	JARE-47 (January), JARE-48 (February-December)	Iwano and Kanao (2009)
Total (N _{DR})	19,145		*re-scaled by Kanao (1995)

and Kanao, 2003; Yoshii and Kanao, 2004; Horiuchi and Kanao, 2005; Doi and Kanao, 2006; Sakanaka, *et al.*, 2007; Chida and Kanao, 2009; Iwano and Kanao, 2009; see Table 1). From 1987 to 1990, particularly, critical re-scaling was conducted, because the tripartite local seismic network was conducted around the Station at the same period and several local events were additionally detected by the network (Kaminuma and Akamatsu, 1992). The additional and modified arrival times for the seismic phases, and epicentral information for the four years, were published by Kanao (1994b).

Teleseismic detectability for the seven years 1987–1993 was previously discussed by Kanao and Kaminuma (1995). Therefore, variations in detection capability in longer term up to two decades are investigated in this study. Several significant characteristics of the detected event information, such as spatial distributions, time variations, and magnitude dependency, are demonstrated in detail by comparison with the analysis on the global network derived from ISC data.

2. Identifying teleseismic events

The detailed procedure for conducting phase identification for teleseismic events is summarized in this Chapter. The initial phases of individual targeted events were carefully picked-up on the analog or the digital records mainly by short-period seismograms (HES) with 1.0 Hz eigen-frequency (Hagiwara, 1958). The earthquake events corresponding to these scaled phases were identified by comparing the estimated

arrival-times calculated by the IASPEI-91 global Earth velocity model (Kennett, 1991) with the observed (scaled) arrival-times. Hypocentral information including origin times were referred from the Preliminary Determination of Epicenters (PDE) or the Quick Earthquake Determination (QED), offered by the National Earthquake Information Center (NEIC), of the USGS.

The onsets of seismic phases were carefully selected within the discrepancy limit of 3.0 s by comparing the calculated travel-times from the IASPEI-91 model with the observed ones. The arrival times of initial phases as well as several other predominant phases such as PKP, PP, S, and SKS were identified; the degree of detection on later phases was dependent on the noise level on the records. Most seismic phases were scaled on the vertical-component seismogram; however, several clear phases were determined on the horizontal components as well. The time accuracy of arrival times was estimated to be ± 0.2 s, caused by human scaling and clock errors in the phase identification procedure.

The numbers of detected earthquakes in the 21 year period from 1987 to 2007 are listed in Table 1. The number detected in each year ranges from 400 to 1700, for a total of 19145. The annually averaged number is more than 900 for the 21 year period. The number of teleseismic events for plotting hypocentral parameters in each figure is 19039, because the body-wave magnitude (M_b) could not be determined for 196

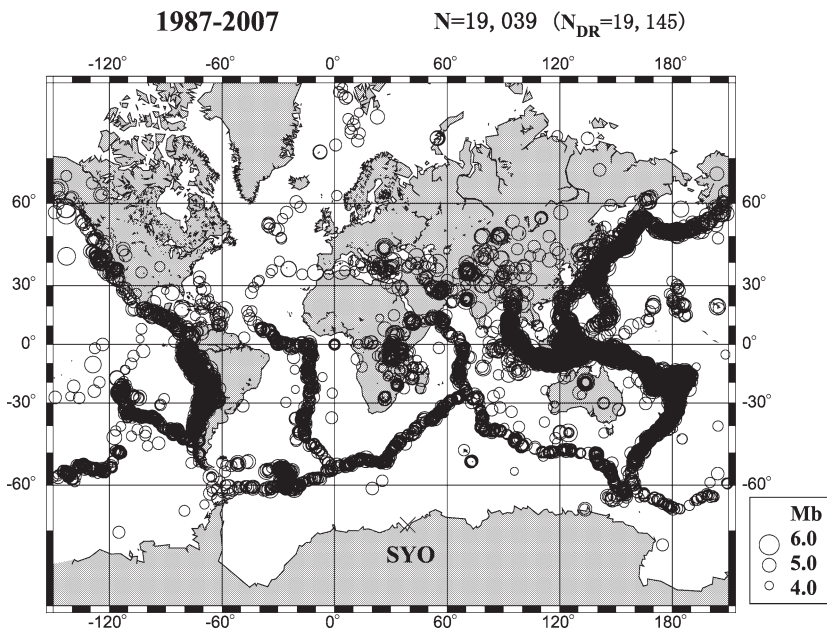


Fig. 1. Epicentral distribution of the teleseismic events detected at Syowa Station in the 21 year period from 1987 to 2007 (Mercator projection). The size of the epicentral circle is proportional to the body-wave magnitude (M_b) determined by USGS. The total number of events (N_{DR}) reported in the Data Reports listed in Table 1 is 19145. Actually the number of teleseismic events plotted on the map is 19039, because of the existence of undetermined M_b for 196 events.

events. The hypocentral distribution for the total 21 year period is shown in Fig. 1. The size of epicentral circles is proportional to M_b reported by USGS.

A small number of local earthquake events with magnitude smaller than 3.0 have been observed at SYO, with their hypocenters around the Lützow-Holm Bay region (*e.g.*, Kanao and Kaminuma, 2006; Kaminuma and Akamatsu, 1992). In this paper, however, we did not treat these local events in detail, but rather summarized the characteristics of relatively large hypocentral distance events which were reported to USGS. Detailed discussion of local events is given in Chapter 8.

3. Spatial distribution of hypocenters

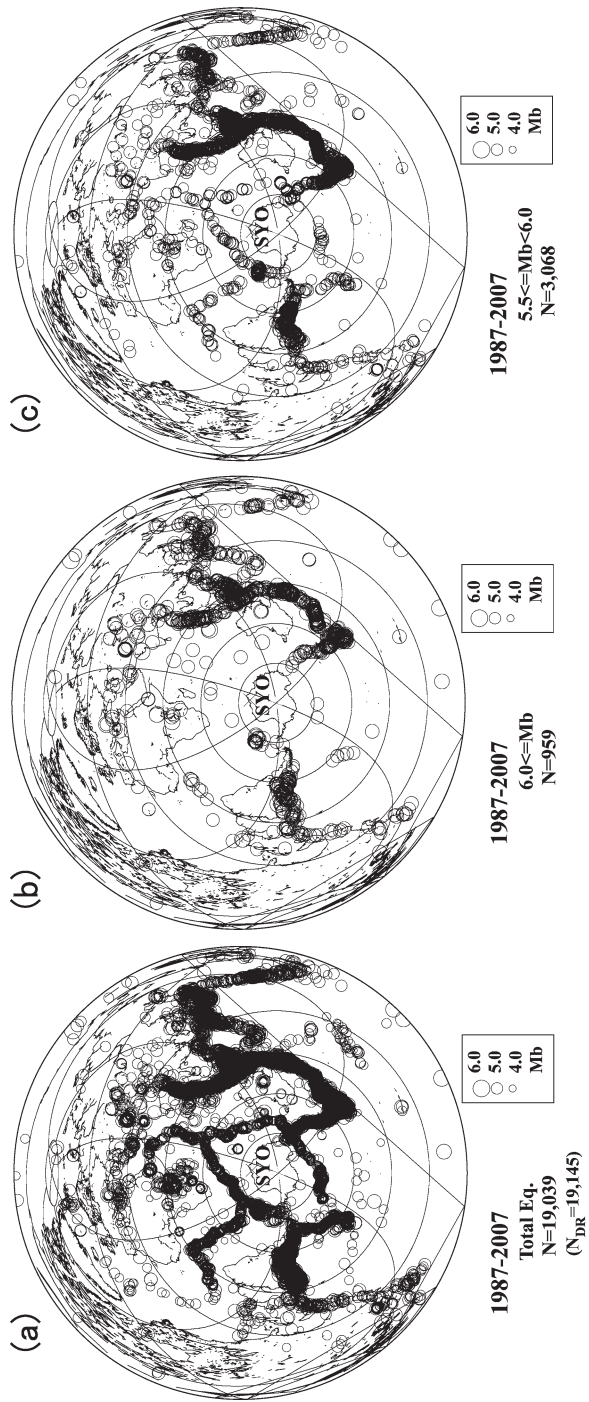
In this section, the spatial distribution on hypocenters is investigated with regard to hypocentral distance and focal depths by dividing into various magnitude ranges. Fig. 2 represents the hypocentral distribution for the 21 year period from 1987 to 2007. All events ($N=19039$ for plotting on the map, $N_{DR}=19145$ for the total number in all of the Data Reports; Table 1), are shown together with five different magnitude range groups.

Magnitude becomes larger as the maximum distance of the detectable epicenters becomes longer. Earthquakes smaller than 4.5 (Fig. 2f), for instance, mainly consisted of large focal depth events in southern hemisphere, along with the shallow depth events around the Antarctic plate. A general pattern of earthquake distribution for all the depth's groups accounts for the approximate location of the plate boundaries.

The relationship between the epicentral distance and the body-wave magnitude (M_b) for 19039 events in the 21 year period is shown in Fig. 3a. The detectable magnitude threshold has minimum values about 3.5 from 60° to 90° , where 80 per cent of the events occurred. On the other hand, the detectable number rapidly decreases particularly at M_b of 5.0, in the shadow zone distance range from 103° to 143° .

Fig. 3b shows the relationship between the epicentral distance and the focal depth for all 19039 events. The maximum number of teleseismic events located in the epicentral distance ranges from 65° to 95° . Since the epicentral distances from 103° to 143° are the shadow zone for seismic body-waves, relatively few initial phases could be identified at Syowa Station. At distances over 140° , PKP phases are principally observed as initial arrival phases. The earthquakes with the distance range more than 150° are located in regions of high northern latitude such as Alaska, the Aleutian Islands, the Kamchatka Peninsula and Svalbard.

The relationship between the focal depth and the body-wave magnitude (M_b) for all 19039 events is shown in Fig. 3c. The detectable magnitude threshold has minimum values around 3.0 at depths shallower than 300 km; teleseismic events with the maximum magnitude (*i.e.*, over 6.5) are mostly detectable at depths shallower than 200 km. The shallower the depths, the larger the detectable maximum with the smaller minimum in M_b ; this evidence is explained by attenuation in seismic waves by considering geometrical spreading in the Earth medium. In the depth range greater than 500 km, moreover, detectable maximum magnitude represents values larger than 6.5; this can be explained by the ease of identification of deep events in the scaling procedure.



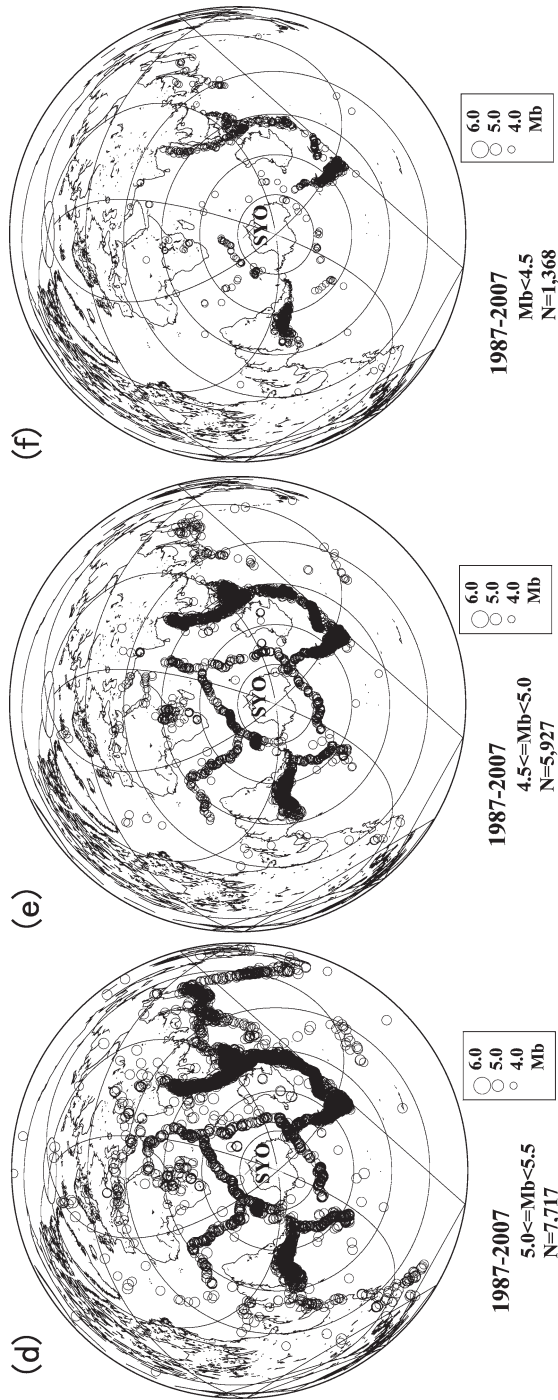


Fig. 2. Epicentral distribution from 1987 to 2007 by the Equi-azimuthal and equi-distant projection of its center at Syowa Station (SYO). The size of the epicentral circle is proportional to the body-wave magnitude (Mb) determined by USGS. (a) for the total number of events ($N=19039$ for plotting hypocenters, $N=19145$ reported by Data Reports); (b) for events with Mb greater than 6.0 ($N=959$); (c) for events with Mb ranging between 5.5 and 6.0 ($N=3068$); (d) for events with Mb ranging between 5.0 and 5.5 ($N=7717$); (e) for events with Mb ranging between 4.5 and 5.0 ($N=5927$); (f) for events with Mb smaller than 4.5 ($N=1368$).

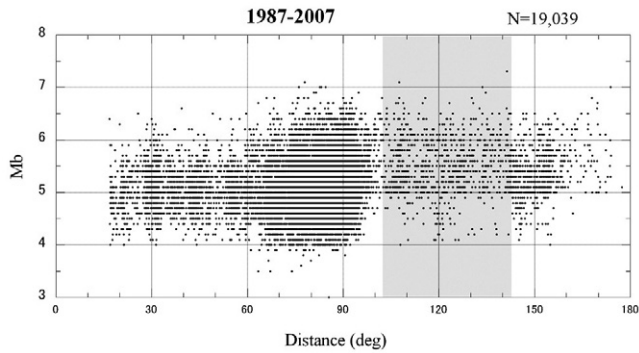


Fig. 3a. Relationship between the epicentral distance (deg) and body-wave magnitude (Mb) for the total 19039 events for the 21 year period of observation. The detectable magnitude threshold has minimum values about 3.5, corresponding to the location of the maximum number of events in the hypocentral distance from 60° to 90°. The shadow zone with hypocentral distance from 103° to 143° is colored gray.

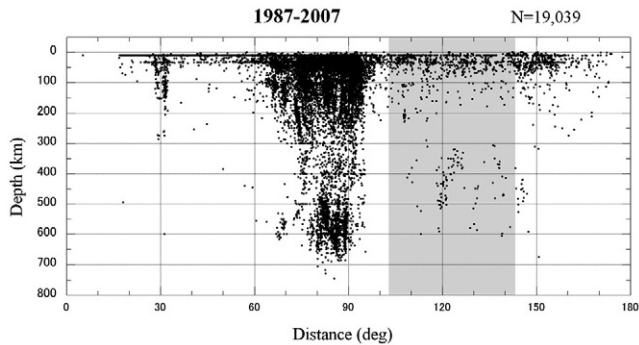


Fig. 3b. Relationship between the epicentral distance (deg) and the focal depth (km) for the total 19039 events. The maximum number of events is located in the distance range from 65° to 95°, where several slab penetrating zones are connected to each other such as the Indonesia region, Tonga and Kermadic Islands, together with the west coast of South America. The seismic shadow zone is clearly indicated in the distance range from 103° to 143° (gray squares). The PKP phases are identified in the distance range of more than 143°.

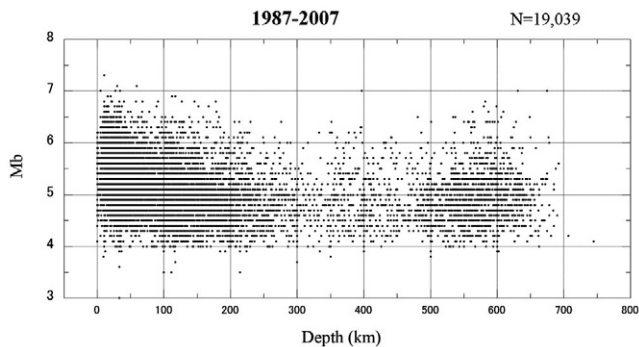


Fig. 3c. Relationship between the focal depth (km) and body-wave magnitude (Mb) for the total 19039 events. The magnitude threshold takes slightly minimum values at shallow depths up to 300 km.

4. Time variations

In this Chapter, time variations in epicentral parameters are investigated in the period from 1987 to 2007. Fig. 4a represents time variations of the body-wave magnitude (M_b) for the 21 year period. The detectable magnitude range varies from 6.5 to 7.0 in maximum, and from 4.0 to 4.5 in minimum, respectively. Time variations with period longer than one year are not so clearly identified at a glance, possibly because the earthquake detection level was not drastically changed throughout the observation period.

When focused on seasonal variations, the austral summer seasons show less teleseismic detectability than the winter seasons throughout the 21 years, because of high noise level in summer due to both natural environmental factors and human activity in the vicinity of the station. The minimum threshold for the detectable magnitude also has a few years of variation ranging from 4.0 to 5.0, which suggests the existence of a relationship between detection capability and other natural parameters (*e.g.*, meteorology, sea-ice spreading area (Ushio, 2003), and other geophysical environmental parameters). More detailed studies on the correlation between M_b variations and environmental parameters are to be done in a further study.

Time variations in the focal depths and epicentral distance during the 21 year observation period are shown in Figs. 4b and 4c, respectively. Although there are variations in the number of detected teleseismic events in individual years (as listed in Table 1), remarkable variations are not recognized in the focal depths during the observation period 1987-2007.

In contrast, the epicentral distance for detected events indicates little change in the shadow zone from 103° to 143° . These shadow zone events seem to include explosion experiments in northern America in the early 1990s in order to produce the first arrival phases. Absence of detection of core phases such as PKIKP in the late 1990s could possibly be dependent on the individual phase identifiers; which implies difficulties in long term observations, particularly in remote places such as Antarctica.

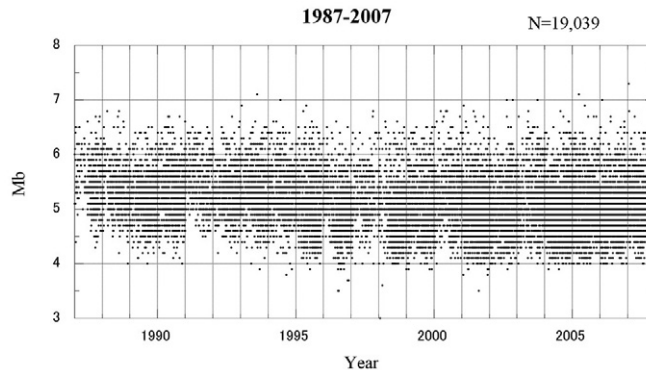


Fig. 4a. Time variations of the body-wave magnitude (M_b) for the 21 year period from 1987 to 2007. The minimum threshold for the detectable magnitude seems to have a seasonal variation ranging from 4.0 to 5.0.

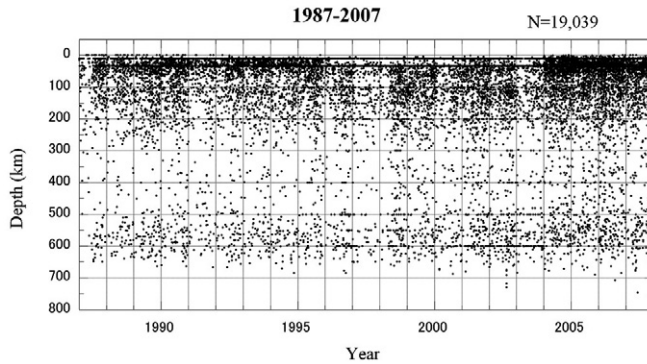


Fig. 4b. Time variations of the focal depth (km) for the 21 year period from 1987 to 2007.

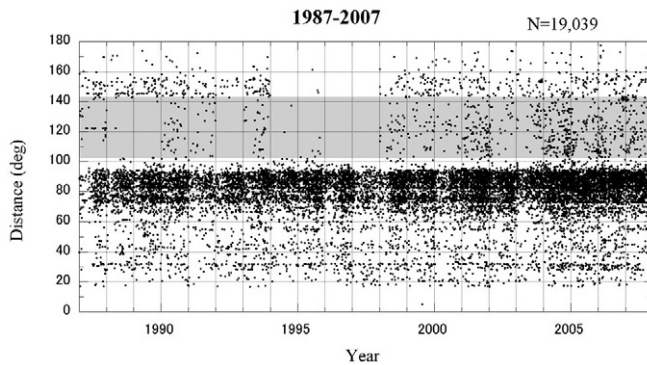


Fig. 4c. Time variations of the epicentral distance (deg) for the 21 year period from 1987 to 2007. The seismic shadow zone is colored gray in the distance range from 103° to 143° .

5. Focal depths and magnitude dependency

In order to clarify the dependence of hypocenters on the focal depths, the magnitude epicentral distribution was classified into three different depth groups by reference to conventional categorization. Fig. 5 presents epicentral maps for events with focal depths shallower than 50 km (Fig. 5(a)), with depths ranging from 50 km to 300 km (Fig. 5(b)), and with depths greater than 300 km (Fig. 5(c)), respectively. Earthquakes deeper than 300 km in focal depth are distributed mainly in the azimuthal range of 70° – 90° (Indonesia region), 130° – 150° (Tonga and Fiji Island regions) and around 250° (South America), as seen in Fig. 5c.

On the basis of classification by focal depth groups, the total cumulative number of detected events the 21 year period against the body-wave magnitude (Mb) is illustrated in Fig. 6a. The number of events in each depth group is marked with an increment of 0.1 Mb. Among the teleseismic events detected at Syowa Station, 58 per cent were “shallow” events with focal depths smaller than 50 km ($N=11156$). In contrast, the “intermediate ($50 \text{ km} < \text{depths} \leq 300 \text{ km}$)” and the “deep (depths larger than 300 km)” events occupy 30 per cent ($N=5776$) and 12 per cent ($N=2204$), respectively.

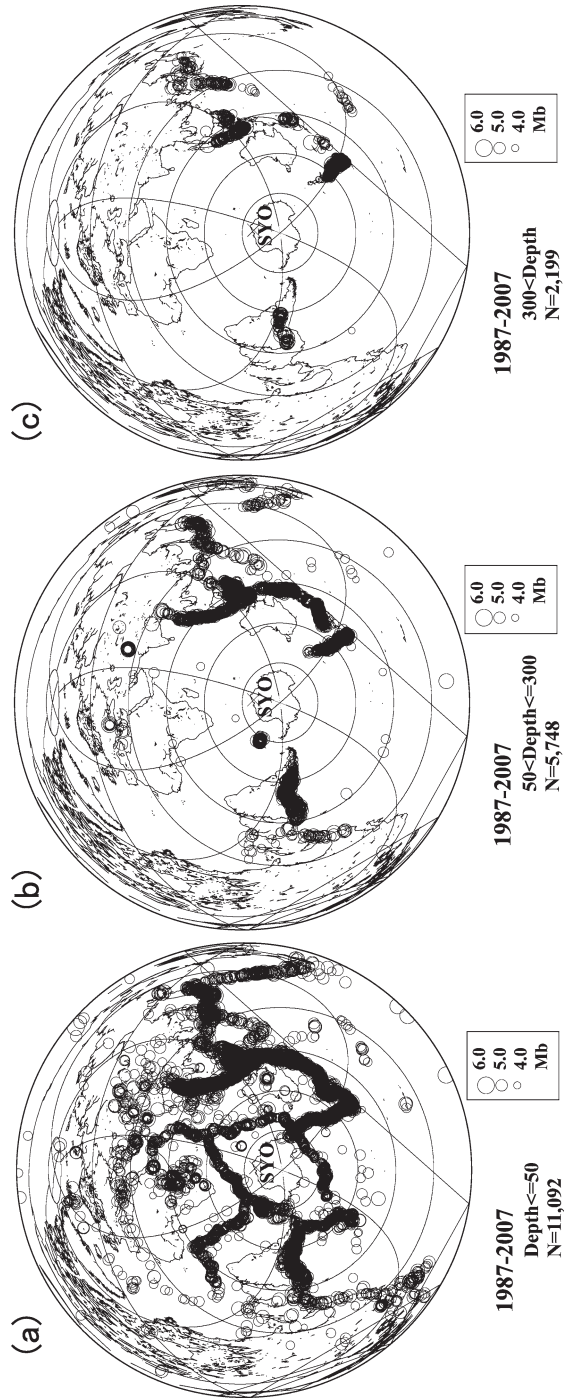


Fig. 5. Epicentral distribution from 1987 to 2007 by the Equi-azimuthal and equi-distant projection of its center at Syowa Station (SYO). The size of the epicentral circle is proportional to the body-wave magnitude (Mb) determined by USGS. (a) for events with depths shallower than 50 km ($N = 11092$); (b) for events with depths ranging from 50 km to 300 km ($N = 5748$); (c) for events with depths greater than 300 km ($N = 2199$).

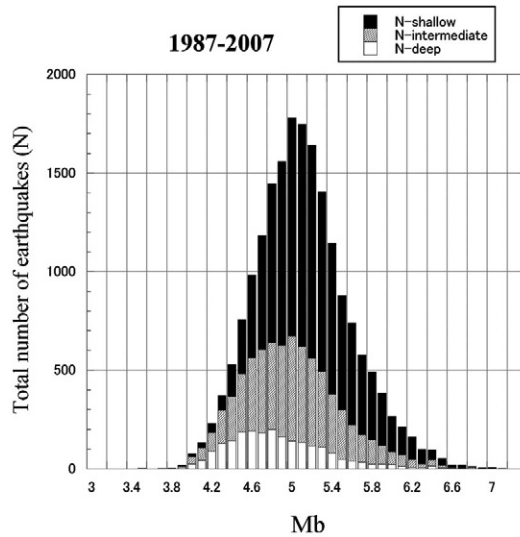


Fig. 6a. Total cumulative number of detected teleseismic events (N) for the 21 year period from 1987 to 2007 against body-wave magnitude (M_b). The number of events in each group is marked with an increment of 0.1 M_b (black columns; shallow events of focal depth shallower than 50 km, hatched columns; intermediate events of focal depth from 50 km to 300 km, white columns; deep events of focal depth larger than 300 km).

The ratio of depth groups derived from the global ISC data indicates that “shallow” events occupy 70 per cent, “intermediate” events 25 per cent, and “deep” events have 5 per cent, respectively (after Ringdal, 1986). This means that the depth’s grouping ratio at Syowa Station is relatively high for “deep” events compared with the global average. In addition, the total numbers of events reported to USGS/NEIC are 350838 “shallow events”, 95122 “intermediate events” and 14982 “deep events”; which give detection ratios at Syowa Station of 3.2 per cent, 6.0 per cent and 14.7 per cent, respectively.

The maximum number of detected events at Syowa Station are located around $M_b=5.0$ for three depth groups, “shallow”, “intermediate” and “total”. In contrast, the maximum number of events occurred around $M_b=4.6$ in the “deep” depth group. This is because the peak position in detected number occurs at relatively smaller M_b values in the “deep” group, as compared with the other groups. This means that the detection capability for the “deep” group is fairly good at Syowa Station for the magnitude range around $M_b\sim 4.0$. The relatively high ratio of about 12 per cent for “deep” events at Syowa Station compared with the global average also indicates that the detection capability for the “deep” group is high.

In order to discuss the annual mean detection capability, we took the average per year of all detected events in the 21 years (Fig. 6b). The peak number of events against magnitude occurred around 5.0-5.1 for the three depth groups except for the “deep” group. The “deep” group, obviously, has peak annual mean values at smaller magnitude around 4.5-4.8. The maximum values for annual mean for the “total” group (*i.e.*, the example of the maximum number group) and the “deep” group (*i.e.*,

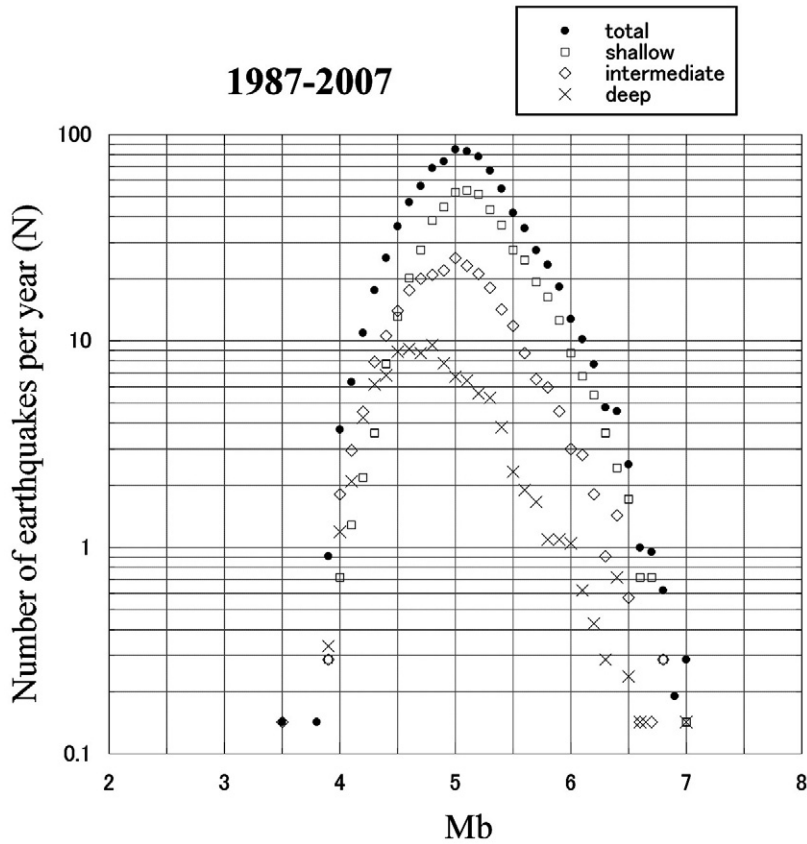


Fig. 6b. Annual mean number of detected teleseismic events (N) for the 21 year period from 1987 to 2007 against body-wave magnitude (M_b). The number of events in each group is marked with an increment of 0.1 M_b (solid circle, total 19039 events; open square, shallow events of focal depth shallower than 50 km; open diamond, intermediate events of focal depth from 50 km to 300 km; cross, deep events of focal depth larger than 300 km).

the example of the minimum number group) are 85 and 10, respectively.

6. Comparison of the b values

Here, we introduce the conventional relationship between magnitude and total number of earthquakes (*i.e.*, the Gutenberg-Richter Law; Gutenberg and Richter, 1944) in order to evaluate the magnitude dependency on the four depth groups under study. Following the modified definition of Ringdal (1986),

$$\text{Log}N = a - b M_b \quad (1)$$

we determine the b values, adopting the average number per year for the detected events as shown in Fig. 6b. In a usual case, we apply the formula to the “cumulative number” greater than M_b . Accordingly, the determined b values in this study are

“pseudo” values as compared with the conventional meaning. In the following discussion, however, we treat “pseudo b values” as simply “ b values” in order to make possible discussion and comparison with the result of Ringdal (Ringdal, 1986).

Incremental recurrence statistics averaged annually for the 21 years of the period, against M_b for four depth groups, are shown in Fig. 7. The slopes of the straight lines adopted for the open squares in each group from (a) to (d) are constrained to determine b values in formula (1). The magnitude range smaller than the peak of $\log N$ values was not used for fitting formula (1) in obtaining b values, because there are not enough detected events in these small magnitude ranges. Moreover, for the three groups except the ‘deep’ group, magnitude greater than 6.5 was not used to determine the b values, because of the insufficient number of events, less than 1 per year (*i.e.*, data with $\log N$ values less than 0 were not used for the fitting). As for the ‘deep’ group, in contrast, the maximum magnitude limit to obtain b values is defined as $M_b=6.0$, for the same reason of insufficient number of events per year of greater magnitude than 6.0.

The b values calculated for the four depth groups under study are listed in Table 2. For comparison, b values of several regional networks are listed (Dean, 1972; Bungum and Husebye, 1974; Chinney, 1978), together with those obtained by using the data of the original ISC bulletin, and maximum-likelihood estimated ones adopting to the same global ISC data (Ringdal, 1986). For the global ISC data, the b values by both analyses indicate a significant difference between 1.40 and 0.90.

The maximum-likelihood estimation was mainly done to improve the magnitude measurements by correcting the network bias problem. The generally reported magnitude tends to become overestimated because information from non-detecting stations for seismic phases is neglected. Then the maximum-likelihood corrected magnitude tends to take smaller values as compared with the original reported ones, which implies smaller b values after correction. Accordingly, the b values by the maximum-likelihood correction for the ISC data (*i.e.*, 0.90) might indicate the same detectability characteristics as the “network magnitude” determined by regional and local seismic networks (averaged in 0.80–1.0).

Table 2. Comparison of the pseudo b values for the four depth groups as classified in the main text. The b values obtained by several regional networks are listed for comparison, together with those obtained by using data from the original ISC bulletin, and the maximum-likelihood b values estimated by Ringdal (1986).

Syowa Station (this study)	pseudo b values
Total depth events; $N=19,039$	1.11
Shallow events; $D < 50$ km, $N=11,092$	1.02
Intermediate events; $50 \text{ km} < D < 300$ km, $N=5,748$	1.03
Deep events; $D > 300$ km, $N=2,199$	0.89
Global network stations (Ringdal, 1986)	
ISC bulletin original	1.40
Maximum likelihood corrected	0.90
Regional array stations (averaged)	
LASA (Dean, 1972)	0.84
NORSAR (Bungum and Husebye, 1974)	0.83
VELA (Chinney, 1978)	0.93

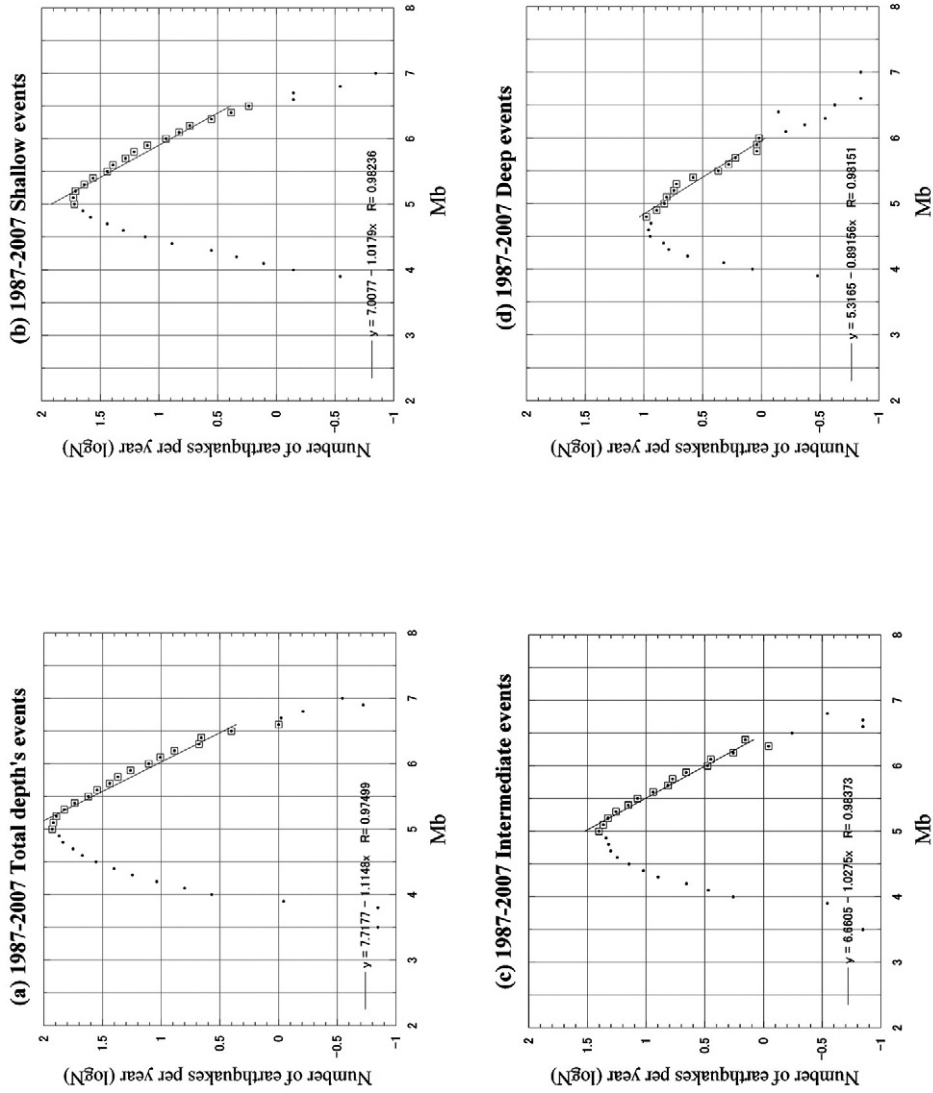


Fig. 7. Incremental recurrence statistics averaged annually for the 21 year period from 1987 to 2007 against body-wave magnitude (Mb). (a) for total number of events, (b) for shallow events, (c) for intermediate events, and (d) for deep events. The slopes of the straight lines adopted for the open squares in each figure were constrained to determine the pseudo b values as discussed in the text.

The b value for the “total”, “shallow” and “intermediate” depth groups under study have ranges in 1.0–1.1, which lie within the range of the other regional networks and two methods which are applied to the global ISC data. The b values for the “deep” group (0.89) are roughly consistent with averaged values of the other regional networks (0.8–1.0) and also the maximum-likelihood estimated values (0.90) for the ISC data. Obviously, the b value for the “deep” group has an apparent difference with the b values of the other depth groups. This is understandable because the position of the peak in the detected number in Mb was relatively smaller (around 4.6) for the “deep” group, in comparison with the other groups (Figs. 6a, 6b). This suggests that the detection capability for the “deep” group has relatively better coverage at smaller magnitude than shallower depth groups.

7. Teleseismic detection capability

The detection capability of the teleseismic events at Syowa Station was first investigated in the 1960s in the early stage of JARE (Kaminuma, 1968). The winter season had higher detection capability, about 5 per cent, than the summer season, which indicates the same characteristics as the seasonal variations in the recent year reported in this study. A succeeding paper in the early 1970s (Kaminuma and Chiba, 1973) demonstrated an improvement of detection capability of about 15 per cent, because the seismic recording system was moved to a new observation hut on Ongul Island with lower noise level.

Subsequently, teleseismic detectability for the seven year period 1987–1993 was investigated by Kanao and Kaminuma (1995). The main features in the spatial distribution of the hypocenters and the focal depths represent almost the same signature as carried out by this study. A longer period for more than two decades until 2007 can be achieved in this study, compared with the previous paper in 1995. Time variations in the hypocentral parameters, the focal depths and the body-wave magnitude represent several years of variations, as discussed in detail in Chapter 4.

The Amundsen-Scott South Pole Station (SPA, now changed to QSPA), for instance, has the highest detection capability among Antarctic stations. (Q)SPA is located at the center of the Antarctic continent, the most remote seismic station from the ocean. Its seismic noise amplitudes caused by oceanic-loading are smaller than at stations along the continental margin. Continuous winter observations at (Q)SPA may contribute to several global science communities, such as natural earthquakes, tsunamis and the Comprehensive Nuclear Test-Ban Treaty Organization (CTBTO) (Butler and Anderson, 2008).

The global detectin capability of the teleseismic events was once evaluated using ISC compiled data, reported from 115 regional networks globally distributed for the ten year period from 1971 to 1980 (Ringdal, 1986). That paper pointed out that the magnitude threshold of earthquake detection increases gradually with increasing southern latitude. The bias problem of network magnitude determination (*i.e.*, the maximum-likelihood estimation described in the previous chapter) is significant at small and intermediate magnitudes, particularly at southern high latitude around Antarctica. The 90 per cent incremental body-wave magnitude threshold was demon-

strated in ranges from 4.2 to 4.8 in the southern hemisphere.

Although there are several broad-band seismic stations in the southern hemisphere by the Federation Digital Seismological Network (FDSN), such as GEOSCOPE (Romanowicz *et al.*, 1991) and PACIFIC21 (Tsuboi, 1995), the detection capability of regional and the local earthquakes should be improved by increasing the number of stations, particularly on the Antarctic continent and in surrounding oceans. Rouland *et al.* (1992) suggested the existence of undetected earthquakes in the ISC bulletin in the southern hemisphere by critically checking the GEOSCOPE data.

8. Discussion

It was generally believed during the International Geophysical Year (IGY) that no large earthquakes occurred in Antarctica. Though the Antarctic was once known as an aseismic region, some significant earthquakes have occurred both on the continent and in the surrounding oceans. Although permanent seismic stations in Antarctica have been operated as a part of the global network, FDSN, since the 1980s, no detailed investigations for mapping local events were carried out until recently (*e.g.*, Kaminuma, 2000; Reading, 2002). Around Syowa Station, for instance, several local earthquakes with magnitude smaller than 3.0 have been detected by regional array stations in the Lützow-Holm Bay region (*e.g.*, Kaminuma and Akamatsu, 1992; Kanao and Kaminuma, 2006).

In recent years, there are several observation reports of local seismicity around Antarctica detected by temporary and permanent station networks. Bannister and Kennett (2002) studied seismicity around the McMurdo Station area detected by temporary broadband stations. They found several interesting features about the local events; that is, the majority events were located along the coast, particularly in the vicinity of large glaciers. They suggested a few reasons for the occurrence of these events: basal sliding of the continental ice sheet, movement of ice streams associated with several scales of glaciers, movement of sea-ice, and tectonic earthquakes. In order to distinguish the actual origins of these events, they mentioned the importance of identifying the earthquake mechanism together with the focal depths. Müller and Eckstaller (2003), in contrast, deployed a local seismic network around Neumayer Station. They determined the hypocenters of tectonic events in the same locality; that is, along the coast and the mid area of the surrounding bay.

By seeing these evidences, several kinds of natural seismic signals were recorded, particularly involving ice-related phenomena. These events are the so-called “icequakes”, which are very frequently generated by glacially related mass movements of ice-sheets, sea-ice, tide-cracks and icebergs (*e.g.*, Wiens *et al.*, 1990; Anandakrishnan and Alley, 1997; Ekström *et al.*, 2006). In spite of the development of local seismic networks during two decades in several regions in Antarctica, we can hardly distinguish between waveforms generated by local tectonic earthquakes and those of ice-related phenomena (*e.g.*, the unknown X-phases are reported by Yamada *et al.*, 2004). These ice-related phenomena seem to have been enhanced by recent global climate change. Accordingly, international cooperation for both the observations

and the data exchange should be encouraged in order to make progress in seismological studies in the southern hemisphere.

Many kinds of archived seismic data (arrival times, hypocenters, waveforms in analog and digital format, and related documents and reports) from observations at Syowa Station have been accumulated and are available from the data library server of NIPR (POLARIS, URL; <http://polaris.nipr.ac.jp/~pseis/syowa>). The seismic waveform data, in particular, are continuously transmitted to NIPR and stored in the data library server, and are accessible upon request via several Internet services.

The present author hereby grants permission for use of these data in scientific papers. Archived data that have passed two years since the JARE observation period are stored and freely available from both the NIPR ftp site and also from the PACIFIC21 data center of the Japan Marine Science and Technology Agency. Then the data will be offered to world seismology data centers, such as Incorporated Research Institute of Seismology/Data Management System (IRIS/DMS).

9. Conclusions

The teleseismic events reported by “JARE Data Reports” for the 21 years 1987–2007 were analyzed to determine spatial and time variations of detection capability at Syowa Station, Antarctica. Several characteristics of the detected events, such as magnitude dependency on spatial distributions, seasonal variations in detectable magnitude with trending in time, and classification into focal depth groups, were demonstrated. Obtained b values for four depth groups take values in 0.89–1.03, comparable with those obtained by regional array stations, and the one estimated to have the maximum likelihood was applied to the global ISC data. Variations in teleseismic detection capability over longer observation terms (seasonal change and a few years of drift) have a possibility to be associated with other environmental data such as weather, sea-ice spreading area, and the other geophysical parameters related to global warming.

Acknowledgments

The author expresses his sincere thanks to Ms. A. Ibaraki of the PDC in NIPR for her great efforts in re-scaling of the major period of our data-set. The author also appreciates to Profs. K. Kaminuma, K. Shibuya, K. Doi, Y. Nogi and Y. Aoyama of NIPR for their valuable advice and discussions in preparing this manuscript.

References

- Anandakrishnan, S. and Alley, R.B. (1997): Tidal forcing of basal seismicity of ice stream C, West Antarctica, observed far inland. *J. Geophys. Res.*, **102** (B7), 15, 183–196.
- Akamatsu, J. and Kaminuma, K. (1989): Seismological bulletin of Syowa Station, Antarctica, 1987. *JARE Data Rep.*, **145** (Seismol. **22**), 73 p.
- Bannister, S. and Kennett, B.L.N. (2002): Seismic activity in the transantarctic mountains—results from a broadband array deployment. *Terra Antarctica*, **9**, 41–46.
- Bungum, H. and Husebye, E.S. (1974): Analysis of operational capabilities for detection and

- location of seismic events at NORSAR. *Bull. Seismol. Soc. Am.*, **64**, 637–656.
- Butler, R. and Anderson, K. (2008): GSN (Global Seismographic Network). *IRIS Ann. Rep.*, 2009, 6–7.
- Chida, K. and Kanao, M. (2009): Seismological bulletin of Syowa Station, Antarctica, 2006. *JARE Data Rep.*, **312** (*Seismol.* **42**), 114 p.
- Chinnery, M.A. (1978): Measurement of m_b with a global network. *Tectonophysics*, **49**, 139–144, doi:10.1016/0040-1951(78)90171-3.
- Dean, W.C. (1972): A geophysical evaluation of the short-period LASA/SAAC system. Virginia, Defense Technical Information Center, Technical rept., AD0745101, SAACR5, 43 p.
- Doi, K. and Kanao, M. (2006): Seismological bulletin of Syowa Station, Antarctica, 2004. *JARE Data Rep.*, **285** (*Seismol.* **40**), 112 p.
- Ekström, G., Nettles, M. and Tsai, V.C. (2006): Seasonality and increasing frequency of Greenland glacial earthquakes. *Science*, **311**, 1756–1758, doi:10.1126/science.1122112.
- Gutenberg, B. and Richter, C.F. (1944): Frequency of earthquakes in California. *Bull. Seismol. Soc. Am.*, **34**, 185–188.
- Hagiwara, T. (1958): A note on the theory of the electromagnetic seismograph. *Bull. Earthq. Res. Inst.*, **36**, 139–164. <<http://hdl.handle.net/2261/11911>>
- Horiuchi, J. and Kanao, M. (2005): Seismological bulletin of Syowa Station, Antarctica, 2003. *JARE Data Rep.*, **280** (*Seismol.* **39**), 54 p.
- Isse, T. and Nakanishi, I. (2001): Inner-core anisotropy beneath Australia and differential rotation. *Geophys. J. Int.*, **151**, 255–263.
- Ito, Y. and Kanao, M. (2003): Seismological bulletin of Syowa Station, Antarctica, 2001. *JARE Data Rep.*, **272** (*Seismol.* **37**), 66 p.
- Iwano, S. and Kanao, M. (2009): Seismological bulletin of Syowa Station, Antarctica, 2007. *JARE Data Rep.*, **313** (*Seismol.* **43**), 101 p.
- Kaminuma, K. (1968): Earthquake detection capability of Syowa Station, Antarctica (Preliminary Reports). *Nankyoku Shiryo* (*Antarct. Rec.*), **33**, 71–80 (in Japanese).
- Kaminuma, K., Eto, T. and Yoshida, M. (1968): Seismological observation at Syowa Station, Antarctica. *Nankyoku Shiryo* (*Antarct. Rec.*), **33**, 65–70 (in Japanese).
- Kaminuma, K. and Chiba, H. (1973): The new seismographic vault and the detection capability of Syowa Station, Antarctica. *Nankyoku Shiryo* (*Antarct. Rec.*), **46**, 67–82 (in Japanese).
- Kaminuma, K. and Ichikawa, N. (1990): Seismological bulletin of Syowa Station, Antarctica, 1988. *JARE Data Rep.*, **151** (*Seismol.* **23**), 78 p.
- Kaminuma, K. and Murakami, H. (1991): Seismological bulletin of Syowa Station, Antarctica, 1989. *JARE Data Rep.*, **160** (*Seismol.* **24**), 66 p.
- Kaminuma, K. and Akamatsu, J. (1992): Intermittent micro-seismic activity in the vicinity of Syowa Station, East Antarctica. *Recent progress in Antarctic earth science*. ed. by Y. Yoshida *et al.* Tokyo, Terra Sci. Publ., 493–497.
- Kaminuma, K. and Nagasaka, K. (1992): Seismological bulletin of Syowa Station, Antarctica, 1990. *JARE Data Rep.*, **172** (*Seismol.* **25**), 106 p.
- Kaminuma, K. and Yamamoto, M. (1993): Seismological bulletin of Syowa Station, Antarctica, 1991. *JARE Data Rep.*, **185** (*Seismol.* **26**), 53 p.
- Kaminuma, K. (2000): A reevaluation of the seismicity in the Antarctic. *Polar Geosci.*, **13**, 145–157.
- Kanao, M. and Kaminuma, K. (1993): Broad-band and wide dynamic-range seismic observations with a Streckeisen seismometer (STS) at Syowa Station, East Antarctica–JARE-33 status report (1992)–. *Nankyoku Shiryo* (*Antarct. Rec.*), **37**, 291–318 (in Japanese).
- Kanao, M. (1994a): Seismological bulletin of Syowa Station, Antarctica, 1992. *JARE Data Rep.*, **192** (*Seismol.* **27**), 69 p.
- Kanao, M. (1994b): Re-scaling of seismic events at Syowa Station, Antarctica, 1987–1990. *JARE Data Rep.*, **200** (*Seismol.* **28**), 212 p.
- Kanao, M. and Kaminuma, K. (1995): Detection capability of earthquakes recorded at Syowa Station, Antarctica, from 1987 to 1993. *Nankyoku Shiryo* (*Antarct. Rec.*), **39**, 156–169.

- Kanao, M. (1999): Seismological bulletin of Syowa Station, Antarctica, 1997, JARE Data Rep., **236** (Seismol. **33**), 65 p.
- Kanao, M., Kaminuma, K., Shibuya, K., Nogi, Y., Negishi, H., Tono, Y. and Higashi, T. (1999): New seismic monitoring observation system and data accessibility at Syowa Station. Nankyoku Shiryo (Antarct. Rec.), **43**, 16-44 (in Japanese).
- Kanao, M., Kubo, A., Shibutani, T., Negishi, H. and Tono, Y. (2002): Crustal structure around the Antarctic margin by teleseismic receiver function analyses. Antarctica at the close of a millennium, ed. by J.A. Gamble, D.N.B. Skinner, S. Henrys. Wellington, Royal Society of New Zealand, 485-491 (Bulletin, **35**).
- Kanao, M. and Kaminuma, K. (2006): Seismic activity associated with surface environmental changes of the earth system, around Syowa Station, East Antarctica. Antarctica: contributions to global earth sciences, ed. by Futterer, D.K., Damaske, D., Kleinschmidt, G., Miller, H. and Tessensohn F. Berlin, Springer, 361-368, doi:10.1007/3-540-32934-X.
- Kanao, M., Doi, K., Sakanaka, S., Uemura, T., Sawagaki, T. and Chida, K. (2006a): Replacement of the seismic monitoring system at Syowa Station, corresponding to the INTERSAT link. Nankyoku Shiryo (Antarct. Rec.), **50**, 287-303 (in Japanese).
- Kanao, M., Nogi, Y. and Tsuboi, S. (2006b): Spacial distribution and time variation in seismicity around Antarctic Plate-Indian Ocean region. Polar Geosci., **19**, 202-223.
- Kennett, B.L.N. (1991): IASPEI 1991: seismological tables. Canberra, Research School of Earth Sciences, Australian National University, 167 p.
- Kobayashi, R. and Zhao, D. (2004): Rayleigh-wave group velocity distribution in the Antarctic region. Phys. Earth Planet. Inter., **141**, 167-181, doi:10.1016/j.pepi.2003.11.011.
- Kuge, K. and Fukao, Y. (2005): High-velocity lid of East Antarctica: evidence of a depleted continental lithosphere. J. Geophys. Res., **110**, B06309, doi:10.1029/2004JB003382.
- Müller, C. and Eckstaller, A. (2003): Local seismicity detected by the Neumayer seismological network, Dronning Maud Land, Antarctica: tectonic earthquakes and ice-related seismic phenomena, IX Int. Symp. Antarct. Earth Sci., programme and abstracts, 236.
- Nakanishi, T. and Kanao, M. (2001): Seismological bulletin of Syowa Station, Antarctica, 1999. JARE Data Rep., **254** (Seismol. **35**), 59 p.
- Nawa, K. and Kanao, M. (1996): Seismological bulletin of Syowa Station, Antarctica, 1994. JARE Data Rep., **210** (Seismol. **30**), 84 p.
- Nawa, K., Suda, N., Satake, K., Fujii, Y., Sato, T., Doi, K., Kanao, M. and Shibuya, K. (2007): Loading and gravitational effects of the 2004 Indian Ocean tsunami at Syowa Station, Antarctica. Bull. Seismol. Soc. Am., **97**, S271-278, doi:10.1785/0120050625.
- Nogi, Y., Negishi, H. and Kanao, M. (1997): Seismological bulletin of Syowa Station, Antarctica, 1996. JARE Data Rep., **229** (Seismol. **32**), 77 p.
- Okano, K. and Kanao, M. (1995): Seismological bulletin of Syowa Station, Antarctica, 1993. JARE Data Rep., **207** (Seismol. **29**), 95 p.
- Reading, A.M. (2002): Antarctic seismicity and neotectonics. Royal Society of New Zealand Bull., **35**, 479-484.
- Ringdal, F. (1986): Study of magnitudes, seismicity and earthquake detectability using a global network. Bull. Seismol. Soc. Am., **76**, 1641-1659.
- Romanowicz, B., Karczewski, J.F., Cara, M., Bernard, P., Borsenberger, J., Cantin, J.M., Dole, B., Fouassier, D., Koenig, J.K., Morand, M., Pillet, R., Prolley, A. and Rouland, D. (1991): The Geoscope program: present status and perspectives. Bull. Seismol. Soc. Am., **81**, 243-264.
- Rouland, D., Condis, C., Parmentier, C. and Souriau, A. (1992): Previously undetected earthquakes in the Southern Hemisphere located using long-period geoscope data. Bull. Seismol. Soc. Am., **82**, 2448-2463.
- Sakanaka, S., Uemura, T. and Kanao, M. (2007): Seismological bulletin of Syowa Station, Antarctica, 2005. JARE Data Rep., **299** (Seismol. **41**), 101 p.
- Seo, N. and Kanao, M. (2002): Seismological bulletin of Syowa Station, Antarctica, 2000. JARE Data Rep., **261** (Seismol. **36**), 51 p.

- Tanaka, T. and Kanao, M. (1997): Seismological bulletin of Syowa Station, Antarctica, 1995. JARE Data Rep., **222** (Seismol. **31**), 103 p.
- Tono, Y. and Kanao, M. (1999): Seismological bulletin of Syowa Station, Antarctica, 1998. JARE Data Rep., **247** (Seismol. **34**), 72 p.
- Tsuboi, S. (1995): POSEIDON (PACIFIC21). IRIS Newsl., **14**, 8–9.
- Tsuboi, S., Kikuchi, M., Yamanaka, Y. and Kanao, M. (2000): The March 25, 1998 Antarctic earthquake: great earthquake caused by postglacial rebound. *Earth Planets Space*, **52**, 133–136.
- Ushio, S. (2003): Frequent sea-ice breakup in Lützow-Holmbukta, Antarctica, based on analysis of ice condition from 1980 to 2003. *Nankyoku Shiryo* (Antarct. Rec.), **47**, 338–348 (in Japanese).
- Usui, U., Hiramatsu, Y., Furumoto, M. and Kanao, M. (2005): Thick and anisotropic D'' layer beneath Antarctic Ocean. *Geophys. Res. Lett.*, **32**, L13311, doi:10.1029/2005GL022622.
- Usui, Y., Hiramatsu, Y., Furumoto, M. and Kanao, M. (2008): Evidence of seismic anisotropy and a lower temperature condition in the D'' layer beneath Pacific Antarctic Ridge in the Antarctic Ocean. *Phys. Earth Planet. Inter.*, **167**, 205–216. doi:10.1016/j.pepi.2008.04.006.
- Wiens, D., Anandakrishnan, S., Nyblade, A. and Aleqabi, G. (1990): Remote detection and monitoring of glacial slip from Whillans Ice Stream using seismic rayleigh waves recorded by the TAMSEIS array. *EOS Trans. AGU*, **87** (**52**), Fall Meet. Suppl., Abstracts 44A-04.
- Yamada, A., Kanao, M. and Yamashita, M. (2004): Features of seismic waves recorded by seismic exploration in 2002: responses from valley structure of the bedrock beneath Mizuho Plateau. *Polar Geosci.*, **17**, 139–155.
- Yoshii, K. and Kanao, M. (2004): Seismological bulletin of Syowa Station, Antarctica, 2002. JARE Data Rep., **274** (Seismol. **38**), 63 p.